Available online at www.sciencedirect.com

ScienceDirect

ELSEVIER

Ceramics International 35 (2009) 2767–2774

CERAMICS
INTERNATIONAL

www.elsevier.com/locate/ceramint

Oxidation behavior of silicon carbide based biomorphic ceramics 7prepared by chemical vapor infiltration and reaction technique

H. Ghanem, E. Alkhateeb, H. Gerhard, N. Popovska *

Department of Chemical Reaction Engineering, University of Erlangen-Nuremberg, Egerlandstrasse 3, D-91058 Erlangen, Germany

Received 2 February 2009; received in revised form 12 February 2009; accepted 13 March 2009
Available online 15 April 2009

Abstract

The oxidation behavior of biomorphic SiC based ceramics with different microstructure and composition was studied at 1450 °C in airflow for 50 h by thermal gravimetric analysis (TGA). SiC with amorphous, coarse grain, crystalline and fine grain crystalline microstructures as well as SiC–Si_3N_4 composite ceramics were processed from paper preforms by chemical vapor infiltration and reaction technique. The ceramics were characterized by X-ray diffraction and scanning electron microscopy coupled with energy dispersive spectroscopy (SEM/EDX) before and after oxidation. The results show that the crystalline SiC with fine grain structure and SiC–Si_3N_4 composite ceramics show very good oxidation resistance at a temperature of 1450 °C.

Keywords: D. SiC; Biomorphic ceramics; SiC–Si_3N_4; Oxidation resistance

1. Introduction

Preparation of biomorphic porous materials from natural products having various compositions and tailored microstructures such as porosity, pore size distribution and morphology have attracted a great deal of attention in the last decades due to the increased number of applications [1]. Silicon based covalent ceramics including SiC and Si_3N_4 are widely studied because of their potential as high temperature structural materials in the development of advanced heat engines, heat exchanger structural components due to their high temperature strength, low coefficient of thermal expansion and high thermal conductivity. Moreover, SiC and SiC–Si_3N_4 possess the highest oxidation resistance among the non-oxide structural ceramics [2]. These materials oxidize to form an adherent SiO_2 protective film on the surface, which shows the lowest permeability to oxygen of all the common oxides [3]. Interesting results concerning oxidation resistance have been obtained with carbon/carbon composites, on which layers of TiC and SiC were deposited. As a result, the number of cracks decreased and oxidation resistance was improved depending on the thickness ratio of TiC to SiC layer as compared with SiC monolayer [4].

Recently, we have published several articles describing the processing of biomorphic ceramics such as SiC, Si_3N_4 and SiC–Si_3N_4 by chemical vapor infiltration and reaction technique (CVI-R) using paper preforms as template [5–7]. SiC with different microstructure like amorphous and crystalline in addition to SiC–Si_3N_4 composites with different composition were obtained. Although biomorphic porous ceramics have much attention there are almost no reports dealing with their oxidation resistance performances up to now. There are several reports in the literature about the oxidation behavior of SiC and Si_3N_4 coatings deposited by plasma spraying, physical vapor deposition, and chemical vapor deposition [8] as well as by tape casting and sintering method [9], which were used as a protective layer on C/C composites [10] and graphite [11]. However, the difficulty in developing effective SiC oxidation protective layers comes from the mismatch of the coefficient of thermal expansion (CTE) between SiC and SiO_2, which leads to crack formation and even debonding under severe oxidation conditions. Some authors tried to solve this problem applying functionally graded coatings [12] or multi-layer coatings [13]. Our approach, studied in this work was to introduce a second phase such as Si_3N_4 in addition to SiC to form SiC–Si_3N_4 composites in order to improve the oxidation resistance minimizing the thermal mismatch with SiO_2

---

* Corresponding author. Tel.: +49 9131 852 7428; fax: +49 9131 852 7421.
E-mail address: n.popovska@rzmail.uni-erlangen.de (N. Popovska).

0272-8842/$36.00 © 2009 Elsevier Ltd and Techna Group S.r.l. All rights reserved.
doi:10.1016/j.ceramint.2009.03.025

layer formed after oxidation. The advantage of Si_3N_4 phase is its very low CTE compared to SiC resulting in a good thermal shock resistance [14].

The present work presents the experimental results on investigation of the oxidation behavior of SiC based biomorphic ceramics at temperature as high as 1450 °C depending on their microstructure and chemical composition.

2. Experimental work

Biomorphic SiC based ceramics were produced by chemical vapor infiltration and reaction technique (CVI-R) using carbonized paper preform as template as well as carbon source for SiC formation in some cases. Paper consisting mainly of cellulose fibers was converted first into carbon biotemplate (C_b) by pyrolysis in inert atmosphere at 800 °C [5], followed by chemical vapor infiltration step with an appropriate precursor system such as MTS/H_2 or $SiCl_4$/H_2 depositing a ceramic or preceramic layer onto carbon fibers. In some cases high temperature treatment was performed as an additional step after CVI, where solid–solid and/or solid–gas chemical reactions took place. The microstructure and the composition of the resulting biomorphic ceramics could be controlled in a wide range varying the precursor system and the conditions during the CVI-R process.

2.1. Investigated materials

2.1.1. Biomorphic SiC ceramics

Biomorphic SiC with different microstructure such as amorphous and crystalline were produced in order to investigate the effect of the phase structure on its oxidation behavior. Methyltrichlorosilane (MTS)/hydrogen mixture was used as a precursor for the CVI to coat the carbon fibers of the template with SiC. Amorphous SiC was produced at infiltration temperature of 950 °C by CVI-I route (Fig. 1) according to Eq. (1). A subsequent thermal treatment in He atmosphere at 1450 °C for 1 h leads to crystallization with the formation of crystalline SiC* with coarse grain structure as indicated by SEM analysis.

The infiltration of the carbon template with MTS/H_2 at higher temperature of 1050 °C according to CVI-II route (Fig. 1) results in deposition of crystalline SiC** with fine grain structure. All CVI experiments to produce biomorphic SiC were performed for 1 h at molar fraction of MTS of 0.08 and α (H_2/MTS) = 3. The residual carbon originated from the template was burned out by oxidation at 750 °C for 5 h in airflow. Fig. 1 presents the flow chart of processing of biomorphic SiC ceramics with different phase structures.

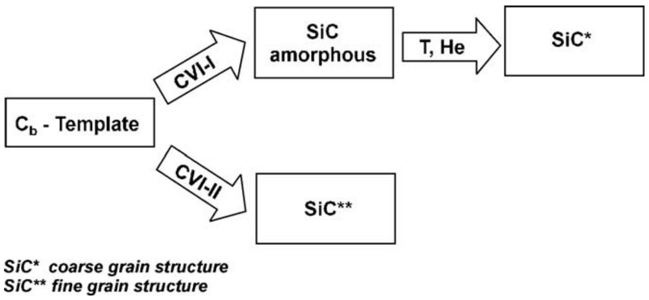

Fig. 1. Flow chart of processing of biomorphic SiC ceramics with different microstructure.

CVI-I

$$C_b + CH_3SiCl_3 \xrightarrow{950\,^{\circ}C,\ H_2} C_b/SiC_{amorph} + 3HCl \xrightarrow{He,\ 1450\,^{\circ}C} C_b/SiC^{*} \qquad (1)$$

CVI-II

$$C_b + CH_3SiCl_3 \xrightarrow{1050\,^{\circ}C,\ H_2} C_b/SiC^{**} + 3HCl \qquad (2)$$

Removal of residual C_b by burning out in airflow

$$C_b/SiC + O_2 \xrightarrow{air,\ 750\,^{\circ}C,\ 5\,h} SiC + CO_2 \qquad (3)$$

2.1.2. Biomorphic SiC–Si_3N_4 composite ceramics

Two different CVI routes with different precursors were used to produce SiC–Si_3N_4 composites with different SiC/Si_3N_4 ratio (Fig. 2).

CVI-III route uses MTS in excess of hydrogen (α = H_2/MTS = 11) at temperature as low as 900 °C to deposit Si rich SiC layer (Si/SiC/C_b) onto the carbon fibers according to Eq. (4) [6]. On the other hand, via CVI-IV route silicon coated carbon template (Si/C_b) was obtained using $SiCl_4$ in excess of hydrogen (α = H_2/$SiCl_4$ = 17) at 900 °C with $SiCl_4$ molar fraction of 0.065 (Eq. (5)). Then, in a second step by submitting the coated Si/SiC/C_b and Si/C_b templates to N_2 atmosphere at 1500 °C for 5 h, composite ceramics with different molar ratio of SiC–Si_3N_4 (9:1) and SiC–Si_3N_4 (4:1), respectively were obtained as a result of solid–solid (C_b–Si) and solid–gas (Si–N_2) reactions. High temperature above the melting point of silicon (1410 °C) and long reaction time is required because of the low diffusion coefficient of the compounds in the solid phase. The residual carbon was also burned out by oxidation at 750 °C in airflow (Eq. (3)).

CVI-III

$$CH_3SiCl_3 + C_b \xrightarrow{900\,^{\circ}C,\ H_2} Si/SiC/C_b + HCl \qquad (4)$$

$$Si/SiC/C_b \xrightarrow{1500\,^{\circ}C,\ N_2} SiC_b/SiC{-}Si_3N_4$$

CVI-IV

$$SiCl_4 + C_b \xrightarrow{900\,^{\circ}C,\ H_2} Si/C_b + 4HCl \qquad (5)$$

$$C_b/Si \xrightarrow{1500\,^{\circ}C,\ N_2} SiC{-}Si_3N_4$$

2.2. Experimental setup

2.2.1. Determination of the composition of the SiC–Si_3N_4 composite ceramics

The composition of SiC–Si_3N_4 ceramics was determined from the mass balance after each processing step (Fig. 2). The amount of the carbon template reacting with silicon to SiC was

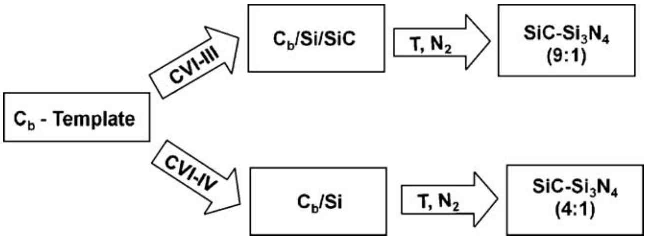

Fig. 2. Flow chart of processing of biomorphic SiC–Si_3N_4 composite ceramics with different composition.

determined as the difference between the initial carbon and the mass loss after the removal of the residual C_b at 750 °C in airflow for 5 h. The amount of the formed Si_3N_4 was estimated from the mass gain after nitridation reaction at 1500 °C for 5 h in N_2 atmosphere.

2.2.2. Isothermal oxidation at 1450 °C

The oxidation behavior of the SiC based biomorphic ceramics at isothermal temperature of 1450 °C was investigated by thermal gravimetric analysis in a thermo balance. The sample was heated in airflow with a heating rate of 5 K/min up to the desired temperature with 50 h dwell at isothermal conditions. Then, the sample was cooled down. Relationships between mass change of the sample and oxidation time were obtained from the isothermal oxidation test. This mass change originated from the oxidation of the SiC, and Si_3N_4, respectively to silica.

2.2.3. Characterization methods

The cumulative mass change of the biomorphic ceramics during oxidation in air was monitored by thermal gravimetric analysis (TGA, Simultan-Thermo-Analysen-Geraet STA 429, Netzsch-Gerätebau, GmbH). The phase analysis of the SiC based biomorphic ceramics was performed by X-ray diffraction (XRD) on a Philips PW 3040 diffractometer. In addition, scanning electron microscopy (SEM) coupled with energy dispersive spectroscopy (EDS) (EDX/SEM Philips XL 30) was used to study the morphology as well as the chemical composition of the ceramics before and after submitting to the high temperature oxidation. Finally, in order to evaluate the mechanical behavior of the sample after high temperature oxidation, maximum bending strength was measured with INSTRON Model 4204 using coaxial double ring bending test with crosshead speed of 0.5 mm/min.

3. Results and discussion

3.1. Oxidation behavior of SiC based biomorphic ceramics at 1450 °C

Biomorphic SiC ceramics with different microstructure show different behavior after submission to isothermal oxidation at a temperature as high as 1450 °C for 50 h duration as shown in Fig. 3. Mass gain of 41% corresponding to 94% conversion of SiC into SiO_2 was obtained for amorphous SiC. According to an extrapolation of the oxidation curve for amorphous SiC, complete conversion into SiO_2 would be achieved by extending the oxidation time up to 192 h.

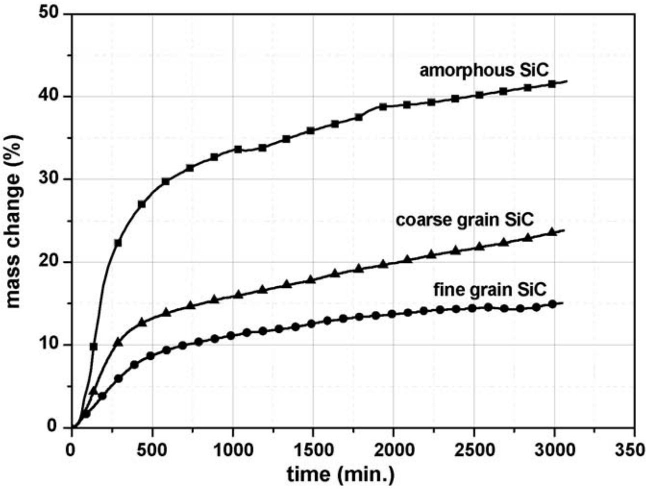

Fig. 3. TGA of SiC with different microstructure during isothermal oxidation at 1450 °C for 50 h.

Crystalline SiC with coarse grain structure produced after high temperature treatment of amorphous SiC (Fig. 1) showed significantly lower mass gain of 23% after oxidation for 50 h corresponding to 82% conversion to silica. The progression of both curves was almost identical, suggesting that the oxidation mechanism was not changed [14].

An interesting behavior can be noticed for crystalline SiC with fine grain structure showing mass gain of 15% corresponding to 76% conversion into SiO_2 after 50 h oxidation. This indicates that the SiO_2 layer formed on the surface was very effective in improving the oxidation resistance of the ceramic.

The high oxidation rate for the amorphous SiC could be explained by its relatively the high specific surface area (SSA) of about 6.1 m^2/g compared to the crystalline samples with SSA of less than 1 m^2/g. The high specific surface area favors the inward diffusion of oxygen to SiC, resulting in an increase in the mass gain as shown in Fig. 3.

The XRD patterns of SiC with different microstructures after isothermal oxidation at 1450 °C for 50 h are shown in Fig. 4. Mainly, SiO_2 in form of α-cristobalite in addition to SiC was detected in all samples. In order to compare the composition of the oxidized ceramics, the ratio of the intensity of SiO_2 and SiC peaks (I_{SiO_2}/I_{SiC}) was estimated from the most intensive peaks of both SiO_2 and SiC at 2θ angle of 21.5° and 35.7°, respectively. The highest ratio of about 4.4 was calculated for crystalline SiC with fine grain structure, whereas for coarse grain structured SiC and amorphous SiC much lower values of 0.75 and 0.94, respectively have been estimated. Therefore, the improvement of oxidation resistance in the case of fine grain crystalline SiC may be due to the retardation of the transport of oxidizing agents through the crystalline dense continuous SiO_2 layer formed on its surface.

In order to compare quantitatively the oxidation resistance of SiC ceramics with different microstructure, the experimental data in Fig. 3 were plotted as square of mass gain per area

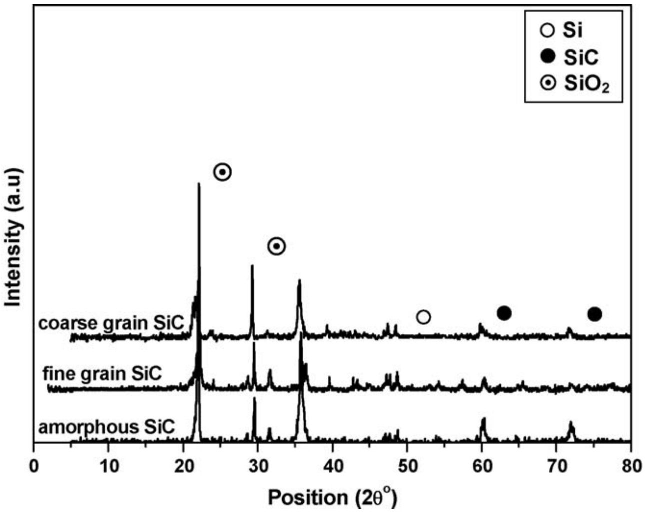

Fig. 4. XRD analysis of SiC with different microstructure after isothermal oxidation at 1450 °C for 50 h.

versus oxidation time (Fig. 5). The data indicate that the oxidation behavior of the ceramics obeys parabolic kinetics according to the following rate equation:

$$\Delta m = (k_p t)^{1/2} \tag{6}$$

where Δm is the mass gain per unit area, k_p the oxidation rate constant and t the oxidation time. The results summarized in Table 1 show that the growth of a surface oxide layer can be divided into two steps. The first step starts with high oxidation rate followed by a second slow oxidation step, which suggest formation of a protective surface layer that inhibits further oxidation. The crystalline SiC with fine grain structure shows an initial oxidation rate of 0.21 min^{-1} at 500 min followed by oxidation rate of 0.064 min^{-1}. Higher initial oxidation rate was estimated for SiC with coarse grain crystalline structure—0.49 min^{-1} and for amorphous SiC—1.77 min^{-1} followed by oxidation rate in the second step of 0.15 min^{-1} and 0.34 min^{-1}, respectively. From these results, it can be concluded that the crystalline SiC with fine grain structure shows the lowest oxidation rate and therefore the best oxidation resistance.

Table 1
Oxidation rate constant k_p of the different silicon carbide based biomorphic ceramics.

Type of ceramics	Oxidation rate, k_p (min^{-1})	
	1 step	2 step
Amorphous SiC	1.77	0.34
Coarse grain crystalline SiC	0.49	0.15
Fine grain crystalline SiC	0.21	0.06
SiC–Si_3N_4 (4:1)	0.41	0.06
SiC–Si_3N_4 (9:1)	0.59	0.16

A second phase of Si_3N_4 was introduced in the SiC in order to produce SiC–Si_3N_4 composites with different composition such as 9:1 and 4:1 using MTS/H_2/N_2 or $SiCl_4$/H_2/N_2 as precursor system, respectively as shown in Fig. 2. The composite ceramic was expected to show improved oxidation resistance at higher temperature compared to pure SiC. Fig. 6 shows the results of TGA of SiC–Si_3N_4 composites with different composition after oxidation at 1450 °C for 50 h. A mass gain of 23% and 17% was measured for SiC–Si_3N_4 ceramics with composition 9:1 and 4:1, respectively. Initially up to 8 h (Fig. 6), both samples show similar oxidation rate of 0.4%/h. After that, it decreases to 0.24%/h and 0.12%/h for (9:1) SiC–Si_3N_4 and (4:1) SiC–Si_3N_4. Therefore, SiC–Si_3N_4 (4:1) composite shows very promising oxidation resistance performance at higher temperatures as it has the minimum mass gain as well as the minimum oxidation rate compared to SiC–Si_3N_4 (9:1) and SiC with different microstructure (Fig. 3).

In Fig. 7 the square of mass gain per area, derived from Fig. 6, is plotted versus the oxidation time. As in the case of SiC (Fig. 5), the oxidation of SiC–Si_3N_4 composite ceramics shows two steps, an initial fast oxidation with high rate constant followed by a slow one (Table 1). Comparing the oxidation rate constants of the different SiC based ceramics in Table 1 it can be concluded, that the composite ceramics with molar ratio 4:1

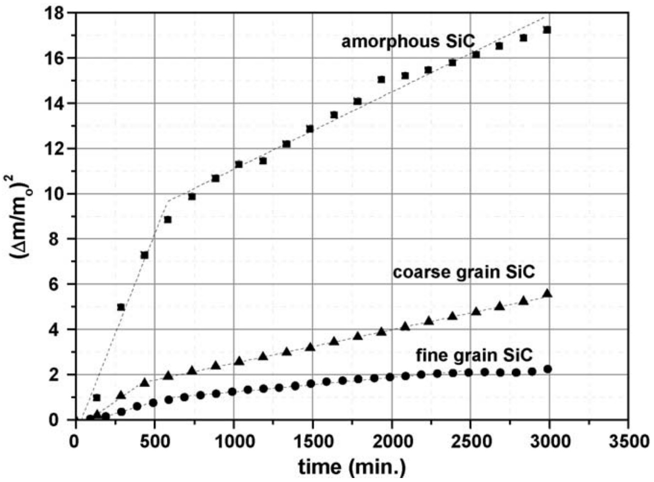

Fig. 5. Relationship between the square of the specific mass as function of the oxidation time at 1450 °C for SiC ceramics.

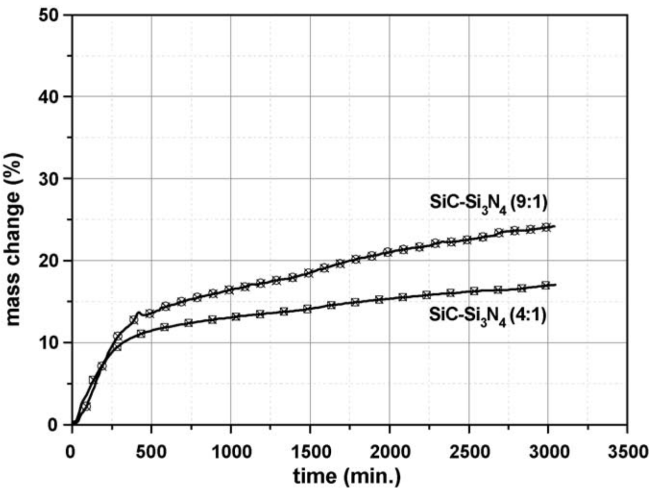

Fig. 6. TGA of SiC–Si_3N_4 after oxidation at 1450 °C for 50 h in airflow.

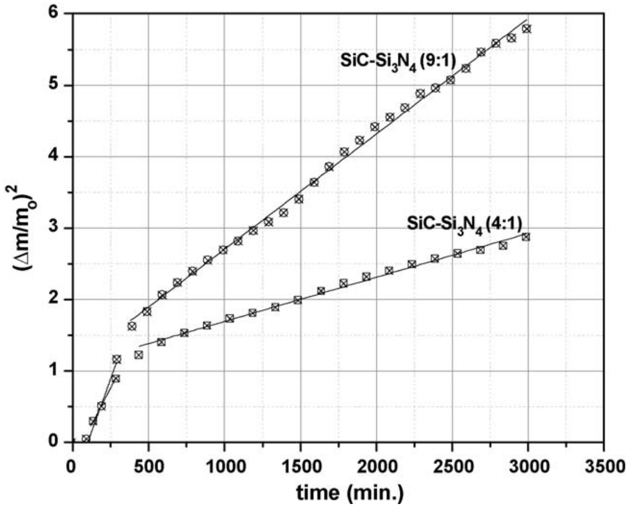

Fig. 7. Relationship between the square of the specific mass as function of the oxidation time at 1450 °C for SiC–Si_3N_4 ceramics.

and the SiC with fine grain microstructure show the best oxidation resistance at high temperature.

3.2. *Morphology of SiC based biomorphic ceramics*

The morphology of the different SiC based biomorphic ceramics before and after isothermal oxidation at 1450 °C was investigated by SEM.

3.2.1. *SiC ceramics with different microstructure*

The morphology of the original SiC ceramics produced by CVI-R technique at different reaction conditions (Fig. 1) is shown in Fig. 8. A big difference between crystalline SiC obtained at high or low temperature can be seen from the micrographs—amorphous samples thermally treated at high temperature shows bigger grains compared with the fine grains in the case of crystalline SiC produced at low temperature. After isothermal oxidation at 1450 °C for 50 h, completely different microstructures were observed (Fig. 9). In the case of amorphous SiC, globules of silica in form of α-cristobalite as detected by XRD were formed because of its melting in addition to rounded spheres of silicon. Deep cracks were formed which serve as a path for oxygen to diffuse to the underlying SiC for further oxidation, which was also confirmed by TGA analysis as shown in Fig. 3. However, different microstructure of SiO_2 film was obtained after oxidation of fine grain crystalline SiC. Homogenous thin film in addition to cracks with 0.5 μm opening were observed, however these cracks were covered with SiO_2, which was formed by reaction of oxygen with the surrounding SiC. As a result, the inward diffusion of O_2 was almost prevented and no further oxidation occurred, resulting in a constant mass gain with the time as shown in Fig. 3. The crystalline SiC with coarse grain structure shows cracks with smaller opening compared to the fine grain crystalline SiC. However, its mass gain after oxidation was higher indicating that this SiC sample has either deep or high number of cracks.

3.2.2. *SiC–Si_3N_4 ceramic composites*

SiC–Si_3N_4 composite ceramics showed different morphology than SiC. As shown in Fig. 10, β-Si_3N_4 with three-dimensional spikes morphology was formed at 1500 °C via CVI routes III and IV (Fig. 2). More homogenous crystalline spikes were formed in the case of nitrided Si to SiC–Si_3N_4 (4:1) than in the case of nitrided Si/SiC to SiC–Si_3N_4 (9:1). The

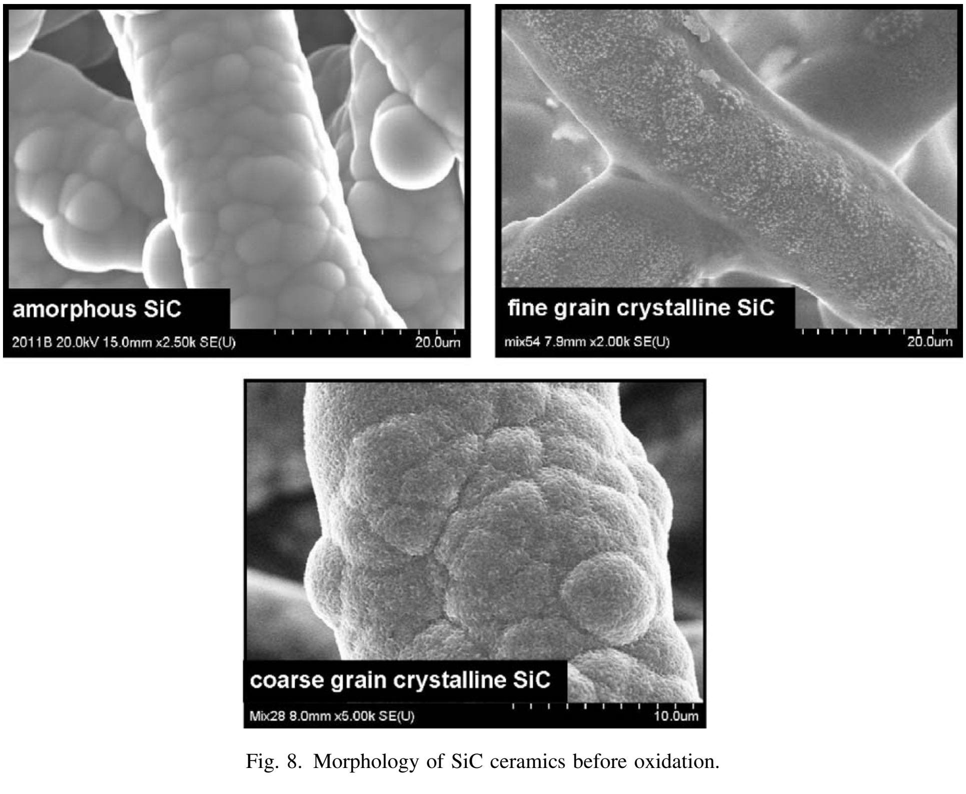

Fig. 8. Morphology of SiC ceramics before oxidation.

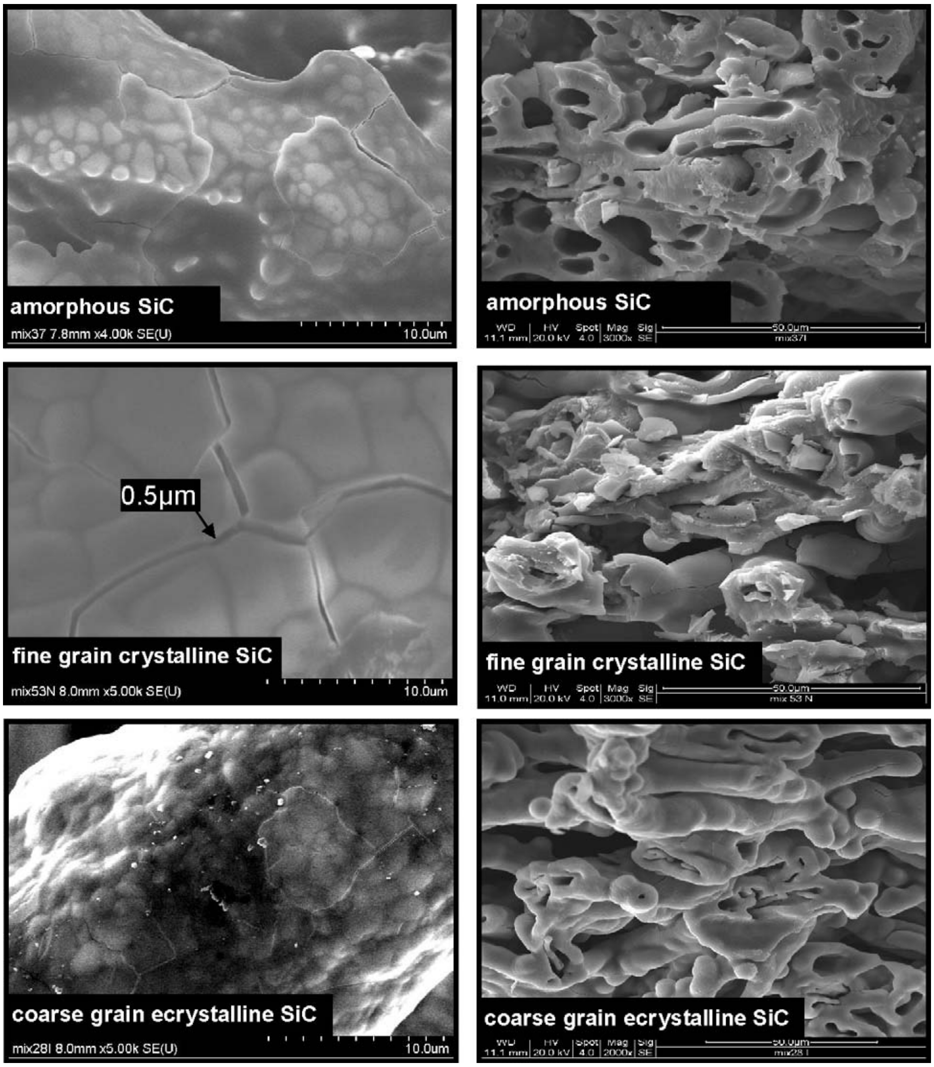

Fig. 9. Microstructure of SiC after isothermal oxidation at 1450 °C for 50 h.

ceramic composite with different composition showed also differences in their morphology after oxidation at 1450 °C for 50 h (Fig. 11). Small cracks with about 0.14 μm opening were formed in the case of SiC–Si_3N_4 (9:1), whereas no cracks were found in SiC–Si_3N_4 (4:1) ceramics. Possible explanation is that the oxidation rate of SiC–Si_3N_4 ceramics decreases with increasing Si_3N_4 content (Fig. 8) due to enhanced grade of crystallization (Fig. 10). This leads to less mass gain and subsequently thinner SiO_2 layer in the case of (4:1) ratio compared to thicker silica film formed after oxidation of SiC–Si_3N_4 (9:1) which then easily causes cracks because of the mismatch between the coefficients of thermal expansion (CTE) of SiO_2 and the non-oxide ceramics. However, the presence of Si_3N_4 in the SiC ceramics was proved to be effective in

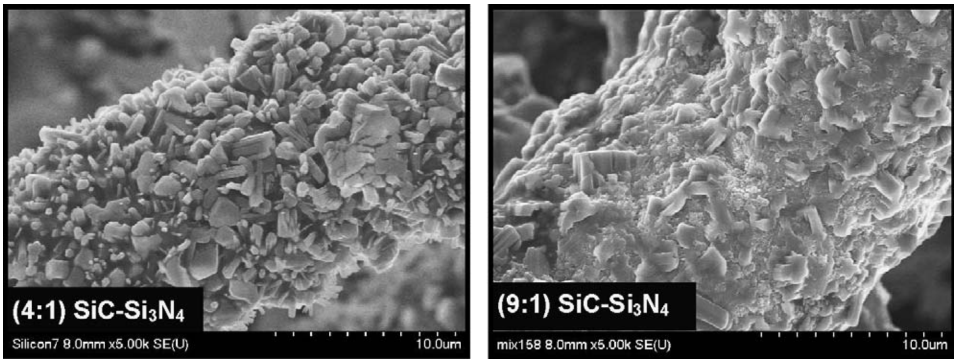

Fig. 10. Morphology of SiC–Si_3N_4 composite ceramics before oxidation.

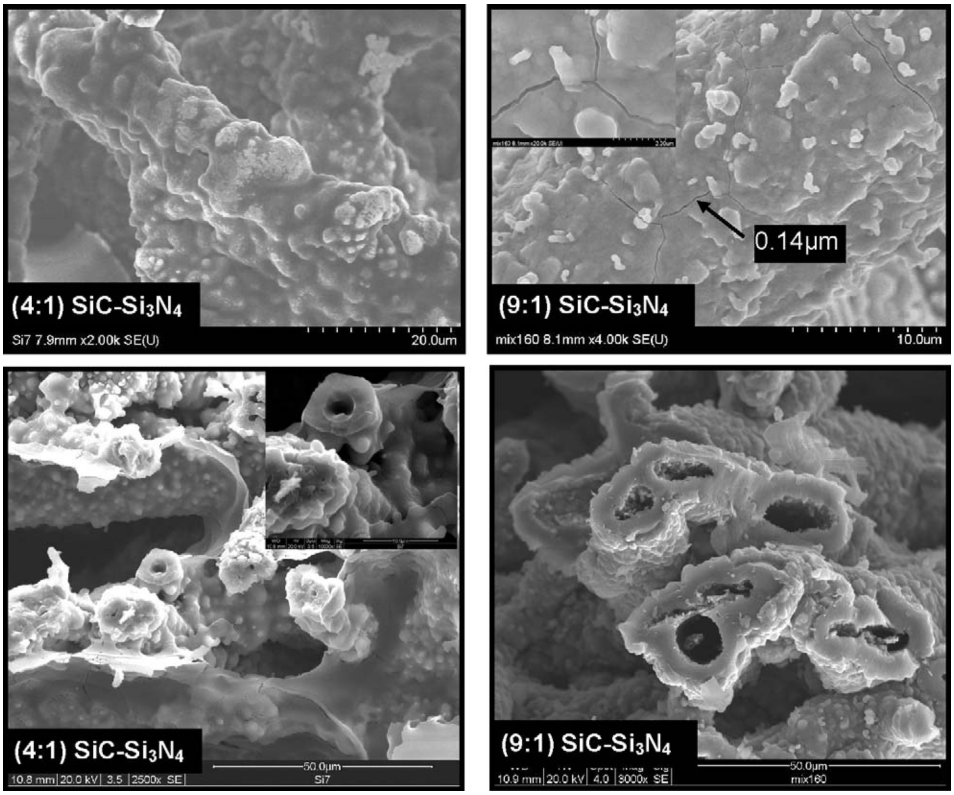

Fig. 11. Morphology of SiC–Si_3N_4 composite ceramics after isothermal oxidation at 1450 °C for 50 h.

minimizing the CTE mismatch with SiO_2 as the value of 3.3×10^{-6}/K for Si_3N_4 is close to the value for SiO_2 and less than that of SiC which has a value of 5×10^{-6}/K [8].

3.3. Bending strength of SiC ceramics after oxidation

The mechanical properties of the biomorphic ceramics are influenced generally by different factors as porosity, surface morphology, grain size as well as residual carbon and silicon in the ceramics after CVI-R processing. All SiC based ceramics investigated in this study have similar porosity of about 50%.

Table 2 presents the bending strength of different SiC ceramics before and after isothermal oxidation. It is observed clearly that the bending strength of the crystalline SiC with coarse grains is lower than this for amorphous and crystalline sample with fine grain structure. The strongest decrease in bending strength after isothermal oxidation at 1450° of about 50% was observed with amorphous SiC, whereas crystalline SiC lost about 30–35% of their strength at these conditions.

Table 2
Bending strength of SiC ceramics after isothermal oxidation at 1450 °C for 50 h.

Type of ceramics	Bending strength	
	MPa	Relative value
Amorphous SiC	20.34	0.53
Fine grain crystalline SiC	19.01	0.70
Coarse grain crystalline SiC	9.10	0.63

4. Conclusions

Biomorphic SiC ceramics with amorphous, coarse grain crystalline or fine grain crystalline microstructure as well as SiC–Si_3N_4 composite ceramics were processed by CVI-R technique varying the precursor system and the process conditions. The effect of the microstructure and composition of the SiC based ceramics on their oxidation behavior in airflow under isothermal conditions at 1450° for 50 h was investigated by TGA analysis.

Parabolic curves with a two-step oxidation behavior were observed. An initial high oxidation rate followed by a low oxidation rate, suggest formation of a protective layer, which prevents further oxidation of the SiC. Amorphous and crystalline SiC with coarse grains show increase in mass change with high oxidation rate while much lower mass change was observed with crystalline SiC with fine grains.

Introducing a second phase of Si_3N_4 to SiC had a significant effect on the mass change after oxidation, microstructure and mechanical properties of the ceramics. In this composite, the oxidation rate decreased with increasing the Si_3N_4 content as well as with the degree of crystallization. Additionally, the presence of a Si_3N_4 phase reduces the thermal expansion mismatch between SiO_2 and SiC resulting in relatively small cracks and well-bonded layers. Composite ceramic with composition 4:1 shows crack free surface after oxidation. However, the bending strength is decreased for all ceramics after isothermal oxidation at 1450 °C due to crack formation, which was severe especially in the amorphous SiC. In conclusions, the oxidation protection of crystalline SiC with fine grain structure as well as SiC–Si_3N_4 (4:1) ceramic composite is adequate for long service times under isothermal conditions in airflow at 1450 °C.

References

[1] R. Studart, T. Gonzenbach, T. Elena, J. Gauckler, A review: processing routes to macroporous ceramics, J. Am. Ceram. Soc. 89 (2006) 1771–1789.

[2] H. Du, R.E. Tressler, K.E. Spear, G. Pantano, Oxidation studies of crystalline CVD silicon nitride, J. Electrochem. Soc. 5 (1989) 1527–1536.

[3] N.S. Jacobson, Corrosion of silicon-based ceramics in combustion environment, J. Am. Ceram. Soc. 76 (1993) 3–28.

[4] C. Kawai, T. Igarashi, Oxidation resistance coating of TiC–SiC system on C/C composite by chemical vapor deposition, Ceram. Soc. Jpn. 5 (1991) 390–394.

[5] D.A. Streitwieser, N. Popovska, H. Gehard, G. Emig, Application of the chemical vapor infiltration and reaction (CVI-R) technique for the preparation of highly porous biomorphic SiC ceramics derived from paper, J. Eur. Ceram. Soc. 6 (2005) 817–828.

[6] H. Ghanem, N. Popovska, H. Gerhard, Processing of biomorphic Si_3N_4 ceramics by CVI-R technique with $SiCl_4/H_2/N_2$ system, J. Eur. Ceram. Soc. 27 (2007) 2119–2125.

[7] H. Ghanem, H. Gerhard, N. Popovska, Paper derived SiC–Si_3N_4 ceramics for high temperature applications, Ceram. Int. 35 (2009) 1021–1026.

[8] D.S. Fox, Oxidation behavior of chemically-vapor-deposited silicon carbide and silicon nitride from 1200 °C to 1600 °C, J. Am. Ceram. Soc. 4 (1998) 945–950.

[9] C. Badini, P. Fino, A. Ortona, C. Amelio, High temperature oxidation of multilayered SiC processed by tape casting and sintering, J. Eur. Ceram. Soc. 22 (2002) 2071–2079.

[10] J. Huang, H. Li, X. Zeng, X. Xiong, Y. Fu, Influence of the preparation temperature on the phase, microstructure and anti-oxidation property of a SiC coating for C/C composites, Carbon 42 (2004) 1517–1521.

[11] N. Bahlawane, A high-temperature oxidation resistance coationg, for graphite, prepared by atmopheric pressure chemical vapor deposition, Thin Solid Films 394 (2001) 297–302.

[12] Y.C. Zhu, S. Ohtani, Y. Sato, N. Iwamoto, Formation of a functionally gradient (Si_3N_4 + SiC)/C layer for the oxidation protection of carbon–carbon composites, Carbon 37 (1999) 1417–1423.

[13] F. Smeacetto, M. Ferraris, M. Salvo, Multilayer coating with self-sealing properties for carbon–carbon composites, Carbon 41 (2003) 2105–2111.

[14] J. Desmaison, High temperature oxidation protection coatings for monolithic or composite ceramics, Werkstoff und Korrosion 41 (1990) 749–750.